IEEE Transaction on Smart Grid. Published online on 11 Mar 2019. DOI: 10.1109/TSG.2019.2904075

Dual-consensus-based Distributed Frequency Control for Multiple Energy Storage Systems

Lantao Xing, Yateendra Mishra, *Member, IEEE*, Yu-Chu Tian, *Member, IEEE*, Gerard Ledwich, *Senior Member, IEEE*, Hongye Su, *Senior Member, IEEE*, Chen Peng, *Senior Member, IEEE*, and Minrui Fei

***Abstract*—Intermittent renewable energy sources are being increasingly integrated into modern power networks. This leads to severe frequency fluctuations in the networks. Energy storage systems can be used for frequency restoration due to their capability to provide in-time active power compensations. This paper deals with the frequency control problem for power systems with multiple distributed battery energy storage systems (BESSs). A dual-consensus-based approach is presented for distributed frequency control. It consists of three main components: tuning of the BESS control gain, design of control signals as inputs to BESSs for proportional use of the preserved energy, and estimation of BESS parameters for control implementation. A static parameter and a time-varying parameter are defined, and their average values are estimated through static average consensus (SAC) and dynamic average consensus (DAC) algorithms, respectively. Case studies are conducted to demonstrate our dual-consensus control approach.**

***Index Terms*—Frequency control; distributed control; battery energy storage systems (BESSs); state-of-charge; consensus**

I. Introduction

Frequency regulation is crucially important for ensuring quality power supply and maintaining the power system stability. In practice, the threshold of frequency deviation from its normal value is ± 0.2 Hz under normal operating conditions. For a sudden loss of power generation of up to $1,800$ MW, the maximum drop of the frequency should be limited to -0.8 Hz. Such a -0.8 Hz drop is required to be restored to the level of -0.5 Hz within 60 seconds [1]. In traditional power systems, independent system operators (ISOs) are responsible for maintaining the frequency stability. An important technique for this purpose is Primary Frequency Control (PFC) aiming to reduce the maximum frequency deviation.

Modern power systems are undergoing transformational changes with the increasing integration levels of traditional centralized power generation, renewable energy sources and energy storage systems. They tend to be distributed in nature with diverse energy sources and storages, as shown in Fig. 1. As renewable energy sources are crucially dependent on environment conditions, they are intermittent and unstable. As a result, the power systems with high levels of renewable energy sources tend to endure severe frequency fluctuations.

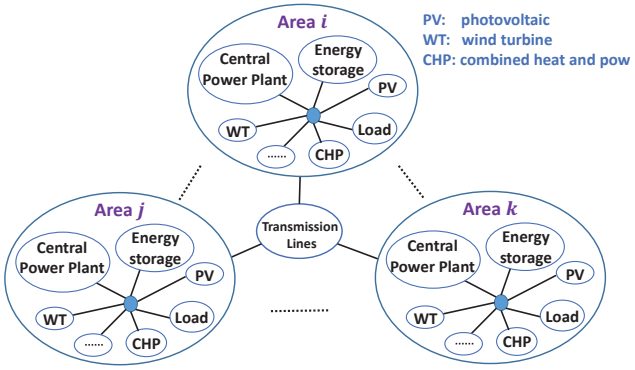

Fig. 1: Power grid with distributed energy storage systems.

Therefore, the frequency regulation becomes more important yet increasingly challenging in modern power systems. For ISOs to meet PFC requirements, both the required volume and associated cost of PFC would be significantly increased due to the limited inertia capability of, say, wind plants. For a power demand of 30 GW, the required primary frequency response is around 1.5 GW in a system without wind generation, but jumps up to more than 3.5 GW in a system with 20 GW absorbed wind generation [2].

Battery Energy Storage Systems (BESSs) integrated in modern low-inertia energy systems are considered to be a potentially effective solution to the improvement of frequency stability [3], [4]. They can provide a fast frequency regulation response and share the load burden of conventional power generation units. With integration of electric vehicles, the volume and cost of PFC can be significantly reduced [2]. A few ISOs, such as Pennsylvania New Jersey Maryland ISO (PJM), New York ISO (NYISO), Midwest ISO (MISO), ERCOT and California ISO (CAISO), have tried to adopt the proportional automatic generation control (AGC) participation strategy, which divides the AGC burden equally among energy storage sources on a per-MW basis [5]. The management of short-term energy resources and dynamic calculation of AGC signals are investigated for frequency regulation enhancement in [6], [7].

Manuscript received ??????, 2018; ??????????. This work was supported by the Australian Research Council through the Discovery Project Scheme under Grant DP160102571 and Grant DP170103305, the National Natural Science Foundation of China (NSFC) under Grant 61833011, and the Ministry of Education of China through the 111 Project Scheme under Grant D18003. Paper no. TSG-??????-2018. (*Corresponding author: Yu-Chu Tian*).

L. Xing, Y. Mishra, Y.-C. Tian and G. Ledwitch are with the School of Electrical Engineering and Computer Science, Queensland University of Technology, GPO Box 2434, Brisbane QLD 4001, Australia.

H. Su is with State Key Laboratory of Industrial Control Technology, Zhejiang University, Hangzhou, 310027, China.

C. Peng and M. Fei are with the Shanghai Key Laboratory of Power Station Automation Technology, School of Mechatronic Engineering and Automation, Shanghai University, Shanghai 200072, China.

Digital Object Identifier ??.????/???.????.???????

10.1109/TSG.2019.2904075

Typically, there are two main approaches for BESS deployment: centralized bulk BESSs with large storage capacity in a few facilities, and distributed BESSs with flexible storage capacity in a large number of facilities. The bulk BESSs have been widely studied for maintaining the power frequency stability. Typical scenarios include power quality enhancement and congestion relief [8], penetration rates and sizing configuration [9]. Recently, distributed BESSs are being increasingly integrated into the power grid. This is due to the following main reasons: (1) Distributed BESSs are more efficient than the bulk BESSs as the energy can be stored or consumed locally rather than transmitted to a remote destination; (2) More and more companies are offering BESSs services. In 2016, about 37 companies placed bids for the tender of enhanced frequency response proposed by the UK National Grid; and (3) More and more residential consumers are installing batteries combining with solar panels.

Therefore, distributed BESSs are expected to play a significant role in improving the power grid performance efficiently and economically. In [10], an BESS coordination strategy is proposed with two operational phases to maximize the profits of integrating BESSs into the ancillary market for frequency support. In [11], comprehensive comparisons of four algorithms are conducted for small-scale distributed BESSs in centralized, decentralized and distributed systems. In [12], the operating and economic benefits of centrally managed BESSs is investigated in an islanded grid. Moreover, a strategy is proposed in [13] which enables BESSs to generate additional revenues from ancillary services such as triad avoidance.

Recently, decentralized droop control is presented to regulate frequency response while maintaining the State-of-Charge (SoC) of each BESS at a desired level for future grid support [14]. The SoC balance issue is addressed in [15] by proper energy sharing through adjusting charging and discharging rates. In [16], a decentralized control approach based on droop control is proposed to achieve SoC balance in an autonomous microgrid. The work in [17] considers distributed control for package-level SoC balance. An SoC-based adaptive droop control is reported in [18] to ensure SoC balance with an adjustable convergence speed. While SoC balance is important, it may not be always appropriate in frequency regulation. The BESSs owned by individuals have their own tasks that may lead to big differences in the SoC values among the BESSs. In this case, it is infeasible to force the SoC values of all BESSs to converge to the same value during frequency regulation.

To maximize the benefits of distributed BESSs for frequency support, it is important for all BESSs to work cooperatively. However, regardless of the above-discussed progress, it is still not well-understood how the SoC status of each BESS should be controlled with the consideration of all other BESSs. Thus, our work in this paper proposes an operating model for multiple BESSs to work collaboratively in frequency regulation. BESS owners reach an agreement with the grid operator on how to use the energy of their BESSs: each BESS reserves a certain (same or different) percentage of its capacity to the grid operator for frequency regulation. For example, the owner of the i-th BESS agrees to reserve 10% of the BESS capacity to the grid operator, requiring that the BESS guarantee its SoC to stay in the range $[SoC_{min,i}+10\%, SoC_{max,i}-10\%]$. Then, the operator can discharge or charge the BESS by up to 10% of the BESS' capacity whenever frequency regulation is needed. During frequency regulation, all BESSs are charged or discharged in proportion to their respective preserved percentages of capacity. The proportional BESS operation ensures no BESS will run out of energy or be fully charged ahead of others, thus always maintaining the maximum possible capacity of frequency regulation from all BESSs.

To ensure our proposed proportional operation of BESSs, this paper further designs a distributed BESS control approach for frequency regulation. The contributions of this paper mainly lie in the following two aspects:

- A dual-consensus-based distributed control of multiple BESSs is designed for frequency regulation. It not only improves the frequency response, but also ensures the proportional use of the preserved capacity of all BESSs regardless of their parameter differences.
- A static BESS parameter and a time-varying SoC parameter, whose average values are respectively estimated by using SAC [19] and DAC [20], are defined for each BESS to enable an actual implementation of our distributed frequency control.

The rest of this paper is organized as follows: Section II presents the formulation of the problem. Then, Section III presents a control strategy with global information. Our dual-consensus- based distributed frequency control is presented in Section IV. Case studies are undertaken in Section V. Finally, Section VI concludes the paper.

II. Problem Formulation

Fig. 2 shows the architecture of our distributed BESS control for frequency regulation of an isolated power system with a reheat thermal generator and N distributed BESSs. All parameters in Fig. 2 are listed in Table I. The lower part of the figure is a conventional generator control loop. As in [4][21][22], an equivalent model is used to describe the isolated power system, and a proportional-integral (PI) controller is used to control the generator.

The upper part of Fig. 2 represents N distributed BESSs and our control system for all these BESSs in the power system.

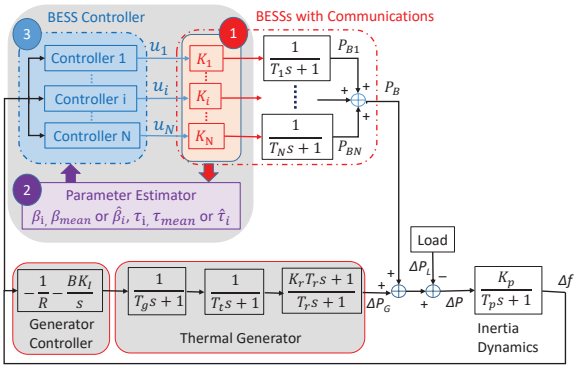

Fig. 2: An isolated power system with multiple BESSs.

TABLE I: Notations and symbols.

a_{ij}	Adjacency element between the i-th and j-th BESSs
B	Thermal generator's frequency bias factor
e	Tracking error vector of DAC
$\mathbf{e}$	Euler's number
$F_i(\cdot)$	Function in controller design for i-th BESS
f, f^{ref}	Frequency and its reference, respectively
$g(\Delta f)$	Function of Δf in BESS controller design
i, j	Subscripts indicating the i-th and j-th BESSs
K_i	Control gain for the i-th BESS
K_i^d, K_i^c	K_i in discharging and charging modes, respectively
K_I, K_p, K_r	Thermal generator's gains
N	The number of BESSs
P_{Bi}	Power input/output of the i-th BESS
P_i^c, P_i^d	BESS power output at Δf_{max}^- and Δf_{max}^+
$P_{min,i}^c, P_{max,i}^d$	The biggest charging and discharging rates, respectively
Q_i	BESS capacity
R	Thermal generator's speed drop
S_i	BESS SoC value (%) relative to the total BESS capacity
$\bar{S}_i$	Preserved BESS capacity (%) for frequency regulation
T_i	BESS time constant
T_g, T_p, T_r, T_t	Thermal generator's time constants
u_i	Control input to the i-th BESS
V	Lyapunov candidate
V_{Bi}, I_{Bi}	BESS output voltage and current, respectively
z, z_1	Intermediate variables
Greek Letters	
β_i	A lumped parameter of the i-th BESS
$\hat{\beta}_i$	Estimation of β_{mean} at the i-th BESS
β_{mean}	Average of all β_i values $\forall\, i \in \{1, \cdots, N\}$
Δf	Frequency deviation
$\Delta f_{max}^+, \Delta f_{max}^-$	Positive and negative thresholds of Δf
$\Delta f_{min}^+, \Delta f_{min}^-$	Positive and negative dead-zone thresholds of Δf
ϵ, ε, γ	Positive design parameters
Γ	$\Gamma \triangleq [1-\tau_1^d, \cdots, 1-\tau_N^d]^T$
μ	Bounded constant
$\hat{\tau}$	$\hat{\tau} \triangleq [\hat{\tau}_1, \cdots, \hat{\tau}_N]^T$
τ_i	Consumed percentage of preserved capacity
τ_i^d, τ_i^c	τ_i in discharging and charging modes, respectively
$\hat{\tau}_i$	Estimation of τ_{mean} at the i-th BESS
τ_{mean}	Average value of all $(1-\tau_i)\ \forall\, i \in \{1, \cdot, N\}$
τ_{mean}^d	τ_{mean} in discharging mode
υ_i	Internal state of DAC

As in [9][23], the input or output power of a BESS, P_{Bi}, can be described by a first-order model as

$$P_{Bi} = \frac{K_i}{1+T_i s} u_i, \ \ i = 1, \cdots, N \tag{1}$$

where i means the i-th BESS, K_i stands for control gain, T_i is time constant, and u_i is the control signal to the BESS.

As shown Fig. 2, our tasks include: 1) to tune BESS control gain K_i; 2) to design BESS controller with output signal u_i as input to the i-th BESS; and 3) to define BESS parameters and their estimation for implementation of the BESS controller. This section will discuss the philosophy in our BESS controller design as well as the criterion of tuning K_i. The BESS controller and parameter estimation will be presented in later sections.

In this paper, $\mathbf{1}_N$ denotes a row vector with all N elements being 1. I_N denotes an $N \times N$ identity matrix. All other notations used in this paper are listed in Table I.

A. The philosophy of BESS controller design

When power generation and load do not match, the frequency f will deviate from its reference f^{ref}, leading to frequency deviation $\Delta f = f^{ref} - f$. In practice, BESSs are expected to act in one of the following three modes to contribute to frequency regulation:

1) If $\Delta f > \Delta f_{min}^+$, then $P_{Bi} > 0$; the BESSs work in discharging mode to inject power to the grid;
2) If $\Delta f_{min}^- \le \Delta f \le \Delta f_{min}^+$ (dead zone), then $P_{Bi} = 0$; all BESSs do nothing in this dead zone; and
3) If $\Delta f < \Delta f_{min}^-$, then $P_{Bi} < 0$; the BESSs work in charging mode to absorb excessive power from the grid.

Thus, a general design of BESS controller is to have the controller output proportional to a function of Δf, i.e,

$$u_i = F_i(\text{System and BESS parameters}) \cdot g(\Delta f), \tag{2}$$

$$g(\Delta f) = \begin{cases} 0, & \Delta f \in [\Delta f_{min}^-, \Delta f_{min}^+] \\ \Delta f - \Delta f_{min}^+, & \Delta f > \Delta f_{min}^+ \\ \Delta f - \Delta f_{min}^-, & \Delta f < \Delta f_{min}^- \end{cases} \tag{3}$$

where $F_i(\cdot)$ is a function of system and BESS parameters. It is seen from Fig. 2 and Eqs. (2) and (3), for $i = 1, \cdots, N$, after K_i is determined, we need to design $F_i(\cdot)$ and also estimate system and BESS parameters in $F_i(\cdot)$ for frequency regulation. If there is no SoC constraint, we may simply set $F_i(\cdot) = 1$.

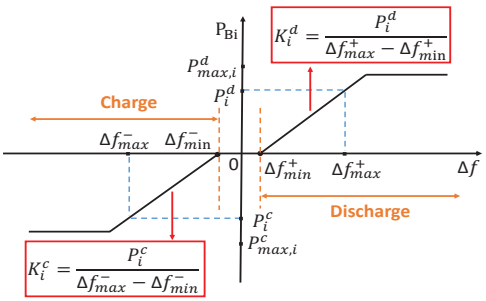

Fig. 3: The $P_{Bi} - \Delta f$ characteristic of BESS control.

B. Criterion to set the gain K_i

It is seen from Fig. 2 and Eqs. (1) to (3) that for a frequency deviation Δf, the corresponding power provided or absorbed by the BESSs is dependent on the gain K_i, $\forall\, i \in \{1, \cdots, N\}$. However, choosing K_i is non-trivial. In the discharging mode, the bigger the value of K_i, the more power the i-th BESS will supply. However, this is subject to a physical constraint of the maximum output power rate. A bigger K_i forces the BESS to work with a faster output power rate, accelerating the degradation of the BESS. On the other hand, if K_i is too small, the benefits of adding the BESSs for better frequency regulation are diminished.

This section presents a method to set the gain K_i based on a $P_{Bi} - \Delta f$ characteristic [24][25], which is shown in Fig. 3. In Fig. 3, p_i^d and p_i^c are the desired power rates of the i-th BESS when Δf hits its positive and negative thresholds, respectively. Meanwhile, $p_{max,i}^d$ and $p_{max,i}^c$ denote the biggest power rates of the i-th BESS in the discharging and charging modes, respectively. Then, from Fig. 3, K_i in Eq. (1) is tuned as

$$K_i = \begin{cases} K_i^d = \frac{p_i^d}{\Delta f_{max}^+ - \Delta f_{min}^+}, \text{ in discharging mode} \\ K_i^c = \frac{p_i^c}{\Delta f_{max}^- - \Delta f_{min}^-}, \text{ in charging mode} \end{cases} \tag{4}$$

C. State-of-charge (SoC) estimation

Let $S_i(t)$ be the SoC of the i-th BESS at time t, $S_i(0)$ be the initial SoC value. Also, let Q_i and I_{Bi} be the BEES capacity and output current, respectively. $S_i(t)$ is estimated by using the basic Coulomb counting method [18][26] as

$$S_i(t) = S_i(0) - \frac{1}{Q_i}\int I_{Bi}dt,\ i = 1, \cdots, N \tag{5}$$

Differentiating both sides of (5) yields $\dot{S}_i(t) = -I_{Bi}/Q_i$. Let V_{Bi} denote the output voltage of battery i. Then, the power output P_{Bi} of the i-th BESS is obtained as $P_{Bi} = V_{Bi}I_{Bi}$. As in [18][26], the output voltage of each battery can be assumed to remain constant for a large range of SoC. Thus, it has

$$\dot{S}_i(t) = -\frac{P_{Bi}}{Q_i V_{Bi}},\quad i = 1, ..., N \tag{6}$$

D. Control objective and constraints

As discussed previously, for $i = 1, \cdots, N$, the ith BESS allocates $\bar{S}_i \in (0, 1)$ of its capacity for frequency regulation. While $\bar{S}_i$ can be different from one BESS to another, the reserved capacity of each BESS is utilized proportionally when frequency regulation starts. Define

$$\tau_i = \begin{cases} \tau_i^d = \frac{S_i(0)-S_i(t)}{\bar{S}_i} - \varepsilon, \text{ in discharging mode} \\ \tau_i^c = \frac{S_i(t)-S_i(0)}{\bar{S}_i} - \varepsilon, \text{ in charging mode} \end{cases} \tag{7}$$

where $\varepsilon > 0$ is a constant to avoid $\tau = 1$ when the reserved energy runs out. In practice, ε should be very small and is set as 10^{-4} in this paper. Thus, τ_i^d and τ_i^c respectively represent the percentages of the reserved energy already consumed in discharging and charging modes.

Corresponding to Components 2 and 3 in the upper part of Fig. 2, the *objective* of this paper is to design a distributed BESS control approach in Eq. (2) for frequency regulation. This is *subject to* the following two constraints, which characterize the proportional use of the preserved percentages of the capacity of all BESSs:

1) If the values of $\tau_i^d(0)$ (or $\tau_i^c(0)$) for $i = 1, \cdots, N$ are the same, then $\tau_i^d(t)$ (or $\tau_i^c(t)$) should be kept the same, implying proportional consumption of the reserved energy across all BESSs; and
2) If the values of $\tau_i^d(0)$ (or $\tau_i^c(0)$) for $i = 1, \cdots, N$ are different, then $\tau_i^d(t)$ (or $\tau_i^c(t)$) should converge proportionally and eventually reach 1 at approximately the same time, indicating that the reserved amounts of energy across all BESSs run out at about the same time.

III. Frequency Control with Global Information

In this section, the control design for Eq. (2) is discussed when all BESS information are available globally. This will facilitate our development later for distributed BESS control without global BESS information. Our discussions in this section are for the discharging mode only. They can be easily extended to the charging mode.

For discharging, it follows from (1), (6) and (7) that

$$\dot{\tau}_i^d = \frac{\beta_i u_i}{1 + T_i s},\ \beta_i \triangleq \frac{K_i^d}{\bar{S}_i Q_i V_{Bi}},\ i = 1, ..., N \tag{8}$$

where β_i is a lumped parameter for the i-th BESS. Since the values of β_i are different in general, the values of $\tau_i^d(t)$ tend to diverge even if the values of $\tau_i^d(0)$ are initially the same for all BESSs. Thus, $F_i(\cdot)$ in Eq. (2) is designed.

For $i = 1, \cdots, N$, to meet the τ_i^d convergence constraints, we design a BESS control in Eq. (2) as

$$u_i = g_i(\beta_i, \beta_{mean}) \cdot f_i(\tau_i^d, \tau_{mean}^d) \cdot g(\Delta f), \tag{9}$$

$$g_i(\beta_i, \beta_{mean}) = \frac{\beta_{mean}}{\beta_i}, f_i(\tau_i^d, \tau_{mean}^d) = \frac{1 - \tau_i^d}{\tau_{mean}^d}, \tag{10}$$

$$\tau_{mean}^d = \frac{1}{N}\sum_{i=1}^{N}(1 - \tau_i^d),\ \beta_{mean} = \frac{1}{N}\sum_{i=1}^{N}\beta_i, \tag{11}$$

where Eq. (11) requires the global information of τ_i^d and β_i for all $i = 1, \cdots, N$, and $g(\Delta f)$ is given in Eq. (3).

Now, let us validate that all values of τ_i^d for $i = 1, \cdots, N$ converge to the same value under our control given in Eqs. (9) to (11). Combining (8) to (10) yields

$$\dot{\tau}_i^d = \frac{\beta_{mean}(1 - \tau_i^d)}{\tau_{mean}^d(1 + T_i s)} g(\Delta f), i = 1, ..., N \tag{12}$$

From the definition of τ_i^d, the changing rate of τ_i^d is determined by the changing rate of S_i. As the BESS output power changes much faster than its SoC does, the effects of T_i and T_j can be neglected in determining the changing rate of τ_i^d. It follows from (12) that for $i, j = 1, \cdots, N$,

$$\frac{\dot{\tau}_i^d}{\dot{\tau}_j^d} = \frac{1 - \tau_i^d}{1 - \tau_j^d} \cdot \frac{1 + T_j s}{1 + T_i s} \approx \frac{1 - \tau_i^d}{1 - \tau_j^d} \tag{13}$$

We have the following theoretical result in Theorem 1.

Theorem 1. *In the discharging mode, for the i-th and j-th BESSs $(i, j = 1, \cdots, N)$ with the controller (9) to (11), if the initial values of $\tau_i^d(0)$ and $\tau_j^d(0)$ are the same, then $\tau_i^d(t)$ and $\tau_j^d(t)$ will remain the same (i.e., the preserved energy will be consumed proportionally); otherwise $\tau_i^d(t)$ and $\tau_j^d(t)$ will converge and eventually reach 1 (i.e., the reserved energy will run out) at the same time.*

Proof: Let $z = \tau_i^d - \tau_j^d$ and $V = \frac{1}{2}z^2$. From Eq. (13)

$$\dot{V} = \frac{1 - \tau_i^d}{1 - \tau_j^d}\dot{\tau}_j^d - \dot{\tau}_j^d = -\frac{\dot{\tau}_j^d}{1 - \tau_j^d}z^2 \tag{14}$$

As $\dot{\tau}_j^d > 0$ and $\varepsilon < 1 - \tau_j^d < 1 + \varepsilon$, we have $\dot{V} \leq 0$. Thus, if $\tau_i^d(0) = \tau_j^d$, $z(t) \equiv 0$, i.e., $\tau_i^d(t)$ and $\tau_j^d(t)$ remain the same.

If $\tau_i^d(0) \neq \tau_j^d(0)$, it is obtained from $\dot{V} = 0$ that $\tau_i^d(t)$ and $\tau_j^d(t)$ will converge towards the same value. Moreover, define $z_1 = \frac{1-\tau_i^d}{1-\tau_j^d}$. z_1 will remain constant because

$$\dot{z}_1 = \frac{-\dot{\tau}_i^d(1 - \tau_j^d) + (1 - \tau_i^d)\dot{\tau}_j^d}{(1 - \tau_j^d)^2} = 0 \tag{15}$$

As a result, $1 - \tau_i^d$ and $1 - \tau_j^d$ will hit zero at the same time, implying that τ_i^d and τ_j^d will reach 1 at the same time. ■

Remark 1. *The control structure (9) has three parts each with its own functions. The first part $g_i(\beta_i, \beta_{mean})$ is to compensate for the effects caused by different BESS parameters β_i. It is*

seen from (12) that with this term, the dynamics of τ_i^d is decoupled from β_i. The second part $f_i(\tau_i^d, \tau_{mean}^d)$ aims to ensure the convergence property of τ_i^d. This is shown in (13) and the proof of Theorem 1. The third part $g(\Delta f)$ responds to Δf by following the $P_{Bi} - \Delta f$ characteristic shown in Fig. 3.

Remark 2. *The control in (9) to (11) requires the global information of τ_i^d and β_i ($i = 1, \cdots, N$). While such global information may be accessible in small-scale systems, it is generally unavailable in large-scale systems with a large-number of geographically distributed BESSs, causing difficulties in implementation of the control strategy. This motivates our work in this paper on distributed BESS control.*

IV. Dual-consensus-based Distributed Control

A. Distributed controller

To alleviate the requirement of global information in control implementation, a distributed control approach is presented:

$$u_i = g_i(\beta_i, \hat{\beta}_i) \cdot f_i(\tau_i^d, \hat{\tau}_i) \cdot g(\Delta f), \tag{16}$$

$$g_i(\beta_i, \hat{\beta}_i) = \hat{\beta}_i/\beta_i,\ f_i(\tau_i^d, \hat{\tau}_i) = (1 - \tau_i^d)/\hat{\tau}_i, \tag{17}$$

where $g(\Delta f)$ is given in Eq. (3), $\hat{\tau}_i$ and $\hat{\beta}_i$ are the estimation of τ_{mean}^d and β_{mean}, respectively. Thus, how to design $\hat{\tau}_i$ and $\hat{\beta}_i$ on each BESS from its own and neighbouring information becomes critical. For distributed BESSs, their communication graph is assumed to be connected and undirected. If the i-th and j-th BESSs are directly connected neighbours, we define a positive adjacency element $a_{ij} > 0$; otherwise, set $a_{ij} = 0$.

By noticing that β_{mean} is a constant while τ_{mean}^d is time varying, a dual-consensus approach is developed to estimate them separately. Specifically, $\hat{\beta}_i$ as an estimation of β_{mean} is obtained by employing SAC [19]. In comparison, $\hat{\tau}_i$ as an estimation of τ_{mean}^d is derived by using DAC [20]. Both SAC and DAC are designed below in details.

B. SAC for $\hat{\beta}_i$ in each BESS

To estimate β_{mean}, we design $\hat{\beta}_i$ as

$$\dot{\hat{\beta}}_i = \sum_{j \in N_i} a_{ij}(\hat{\beta}_j - \hat{\beta}_i),\ \hat{\beta}_i(0) = \beta_i,\ i = 1, \cdots, N \tag{18}$$

We have the following Lemma:

Lemma 1. *The DAC algorithm (18) guarantees that $\hat{\beta}_i, i = 1, ..., N$, will globally and exponentially converge to β_{mean}.*

Proof: The proof is similar to the proof of Theorem 5 in [19] and thus is omitted here. ∎

Remark 4. β_{mean} is a constant. Thus, when $\hat{\beta}_i$ converges to β_{mean} with a satisfactory error, Eq. (18) can stop running.

C. DAC for $\hat{\tau}_i^d$ in each BESS

To estimate time-varying τ_{mean}, we design $\hat{\tau}_i$ as

$$\begin{cases} \hat{\tau}_i = \upsilon_i + 1 - \tau_i^d,\ i = 1, ..., N, i \neq j \\ \dot{\upsilon}_i = -\gamma \upsilon_i + \sum_{j \in N_i} a_{ij}(\hat{\tau}_j - \hat{\tau}_i) \end{cases} \tag{19}$$

where υ_i is an internal state, and $\gamma > 0$ is a constant.

Define $\hat{\tau} = [\hat{\tau}_1, ..., \hat{\tau}_N]^T$ and $\Gamma = [1 - \tau_1^d, ..., 1 - \tau_N^d]^T$. From (7), τ_i^d must be bounded. Moreover, as $\dot{\tau}_i^d = -\dot{S}_i/S_i$, $\dot{\tau}_i^d$ is bounded. It is concluded that $||\gamma\Gamma + \dot{\Gamma}|| \leq \gamma||\Gamma|| + ||\dot{\Gamma}|| \leq \mu$ where μ is a bounded constant. Define tracking error vector

$$e = \hat{\tau} - \mathbf{1}_N \mathbf{1}_N^T \Gamma/N = \hat{\tau} - \mathbf{1}_N \tau_{mean}^d \tag{20}$$

Then, we have the following Lemma:

Lemma 2. *If the parameters are chosen as $\gamma > 0$, $\epsilon > 0$, $\mathcal{L} + \mathcal{L}^T \geq 2\epsilon\Pi$, and $\Pi = I_N - \mathbf{1}_N \mathbf{1}_N^T/N$, then the DAC algorithm (19) guarantees that $||e||$ will exponentially converge to the set $\Omega_e = \{e \mid ||e|| \leq \frac{\mu}{\gamma + \epsilon}\}$ which can be made arbitrarily small.*

Proof: From Theorem 4 in [20], it can be obtained that

$$\begin{aligned} ||e(t)|| \leq & \frac{1}{\sqrt{N}} |\mathbf{1}_N^T \upsilon(t_0)| \mathbf{e}^{-\gamma(t - t_0)} \\ & + |\Pi \hat{\tau}(t_0)| \mathbf{e}^{-\frac{1}{2}(\gamma + \epsilon)(t - t_0)} + \mu/(\gamma + \epsilon) \end{aligned} \tag{21}$$

Therefore, $||e||$ will exponentially converge to Ω_e. As μ is bounded, by setting a big ϵ, which indicates big a_{ij} to make $\mathcal{L} + \mathcal{L}^T \geq 2\epsilon\Pi$ hold, Ω_e can be made arbitrarily small. ∎

D. Analysis of control performance

Eqs. (16)-(19) form our dual-consensus-based distributed frequency controller. We have the following theoretical result:

Theorem 2. *With the distributed control approach (16)-(19), the results in Theorem 1 still hold.*

Proof: From (8), (16) and (17), it is obtained that

$$\frac{\dot{\tau}_i^d}{\dot{\tau}_j^d} = \frac{1 - \tau_i^d}{1 - \tau_j^d} \frac{\hat{\tau}_j}{\hat{\tau}_i} \frac{\hat{\beta}_i}{\hat{\beta}_j},\quad i, j = 1, \cdots, N \tag{22}$$

As both $\hat{\tau}_i$ and $\hat{\beta}_i$ converge much faster than τ_i^d, we have

$$\dot{\tau}_i^d/\dot{\tau}_j^d \approx (1 - \tau_i^d)/(1 - \tau_j^d),\quad i, j = 1, \cdots, N \tag{23}$$

Thus, Theorem 2 can be proved by following the analysis in the proof of Theorem 1. ∎

V. Case Studies

To demonstrate our dual-consensus-based distributed control approach, two case studies are conducted. The first one considers the case where the generator has sufficient generation capability for load disturbances. In this case, the BESSs help in improving the frequency response while meeting the proportional use constraint. The second case study investigates a scenario where the generator has insufficient generation capability. Thus, the BESSs are required to work for a longer time for maintaining the frequency stability. In both case studies, our dual-consensus control approach is compared with two recent and relevant methods [13][24] in which the $P_{Bi} - \Delta f$ characteristic is also adopted.

In our case studies, 10 distributed BESSs with the communication graph shown in Fig. 4 are integrated into an isolated power system. Their parameters and other system parameters are listed in Table II. The control period is set as $1/60$ s, which is the sampling rate of phasor measurement units (PMUs) in the current industry practice. While we have

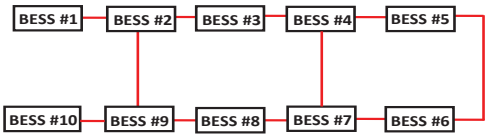

Fig. 4: BESSs communication graph.

TABLE II: BESS parameters and other system parameters.

BESS i	T_i (s)	P_i^d/P_i^c (MW)	Q_i (MWH)	V_{Bi} (KV)
1	0.5	1	1	2
2	0.4	0.9	0.88	2.2
3	0.9	0.98	0.81	1.8
4	0.7	1.12	0.99	2.1
5	0.8	1.08	0.96	1.6
6	0.2	0.95	0.93	1.7
7	0.6	1.2	1.16	2
8	0.5	1.15	1.17	2.3
9	0.7	0.85	0.99	1.9
10	0.3	0.8	0.96	2
Power generator parameters [21]: Power capacity: 1 pu = 1,000 MW				
$K_p = 120$ Hz/pu MW		$T_p = 20$ s	$K_r = 0.5$ s	
$B = 0.425$ pu MW/Hz		$T_r = 10$ s	$T_t = 0.3$ s	
$R = 5.6$ Hz/pu MW		$T_g = 0.08$ s	$K_I = 0.033$	

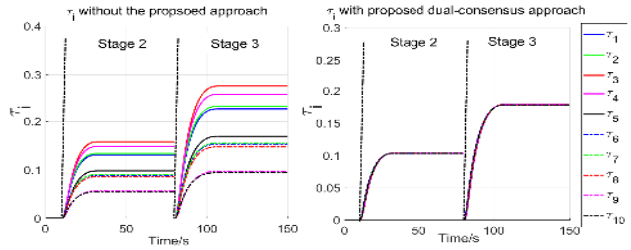

Fig. 5: Case study 1 - performance of τ_i.

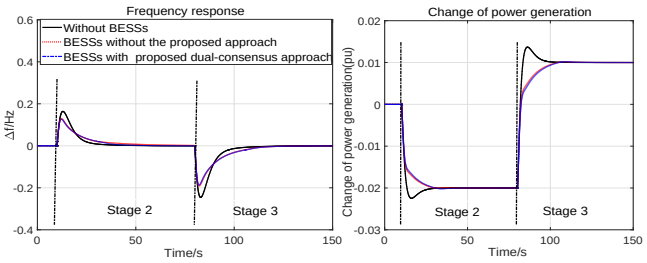

Fig. 6: Case study 1-frequency and power generation change.

used periodic control in our case studies to demonstrate the advantages of our approach, event-triggered control [27] can also be employed in control implementation to reduce the communication traffic.

Similar to [9], $\Delta f^+_{min} = -\Delta f^-_{min} = 0.02Hz$ and $\Delta f^+_{max} = -\Delta f^-_{max} = 0.2$ Hz are set. The BESSs are allowed to work in the range $[10\%, 90\%]$, and the initial SoC values for the 10 BESSs are respectively set as 65%, 60%, 58%, 50%, 70%, 62%, 49%, 53%, 68% and 75%. For each BESS, the maximum allowed rate of power injection into the grid is 0.002 pu.

A. Case study 1: Sufficient generation capability

In this case study, it is assumed that $\bar{S}_i = 1\%$ for $i = 1, 2, 3, 4$, $\bar{S}_i = 1.5\%$ for $i = 5, 6, 7, 8$, and $\bar{S}_i = 2\%$ for $i = 9, 10$. The power system undergoes three stages:

Stage 1: 0-10 s, The system operates in the steady state;
Stage 2: At 10 s, a 0.02pu load is taken off from the grid;
Stage 3: At 80 s, a 0.03pu load is added to the grid.

The advantage of our distributed BESS control approach for frequency regulation is shown in Fig. 5-8. As shown in Fig. 5, the values of τ_i for all BESSs with our approach remain almost the same, implying perfect proportional use of the preserved BESS capacity among all BESSs. This implies that the BESSs always maintain the maximum possible capacity for frequency regulation. In comparison, the values of τ_i of all BESSs diverge over the time for the method without our proposed approach, indicating the risk of reduced capacity from the BESSs for frequency regulation.

In Fig. 6, without BESSs for frequency regulation, for a 0.03 pu load change at 80 s, Δf will reach -0.25 Hz, violating the normal operating condition. In comparison, with the help of BESSs for frequency regulation, Δf can be compressed to within -0.2 Hz. As shown in Fig. 6, our proposed approach can guarantee the frequency response similarly well with the method without our distributed control approach. Fig.7 shows the performance of SAC and DAC, while Fig.8 compares the BESS output with and without our proposed approach.

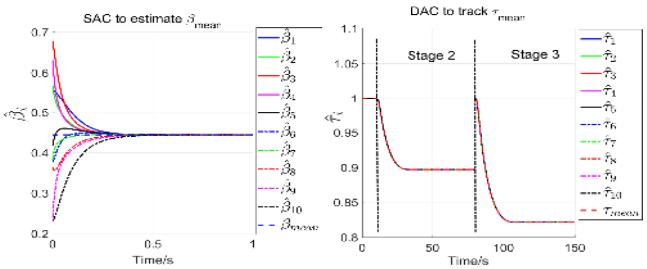

Fig. 7: Case study 1 - performance of SAC and DAC.

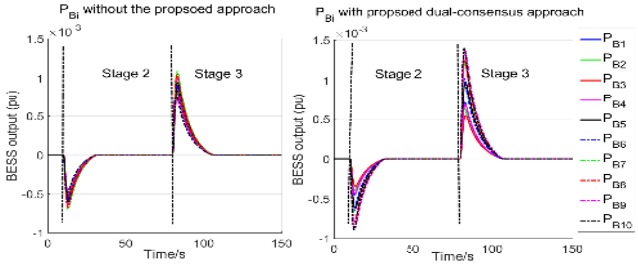

Fig. 8: Case study 1 - BESS output.

B. Case study 2: insufficient generation capability

A 0.02 pu load is added to the grid, while the generator can only generate 0.01 pu additional power, indicating a gap of 0.01 pu. In addition, a generation rate constraint of $3\%/\min$ (i.e. 0.0005pu/s) [21] is imposed to power generation to ensure the safe operation of power generation equipment. The 10 BESSs are divided into two groups, and the allocated energy is $\bar{S}_i = 5\%$ for the first five BESSs while $\bar{S}_i = 10\%$ for the other BESSs. The initial τ_i^d values of the 10 BESSs are set as 10%, 5%, 15%, 0%, 6%, 0%, 2%, 20%, 18%, and 3%, respectively. The simulation results are shown in Figs. 9-11.

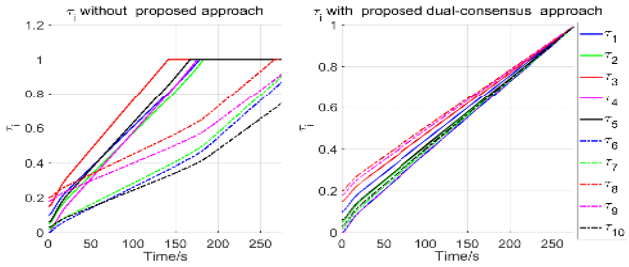

Fig. 9: Case study 2 - performance of τ_i.

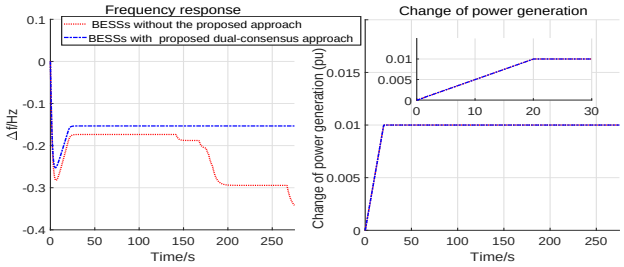

Fig. 10: Case study 2-frequency and power generation change.

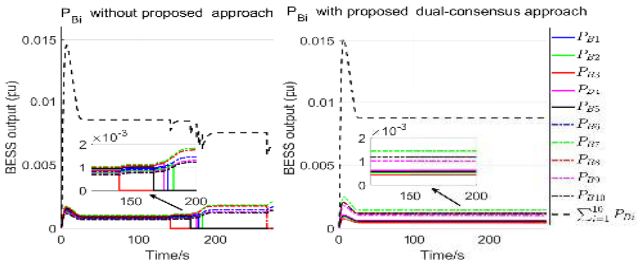

Fig. 11: Case study 2 - BESS output.

As shown in Fig. 9, the values of τ_i for all BESSs converge when our approach is employed but diverge when our approach is not used. The divergence of the values of τ_i for all BESSs means some BESSs will be exhausted much earlier than others. This is verified by the BESS power output shown in Fig. 11. It is seen from Fig. 11 that our approach maintains proportional power outputs among all BESSs for over 250 s. In comparison, without our approach, some BESSs are exhausted much earlier than others after about 120 s.

The proportional use of the preserved capacity of all BESSs by our proposed approach always maintains the maximum possible capacity from all BESSs for frequency regulation, and consequently serves frequency regulation longer. Fig. 10 shows that the addition of the 0.02 pu load causes Δf to go beyond -0.2 Hz. With the help of BESSs, both methods with and without our control approach are able to bring Δf back to within -0.2 Hz. However, the peak value of Δf is compressed by using our approach in comparison with the method without using our approach.

It is also observed from Fig. 10 that our approach maintains the Δf within -0.2 Hz for over 250 s. In comparison, the method without using our approach fails to do so shortly after about 170 s, from which Δf drifts away quickly to about -0.3 Hz, significantly violating the normal operating condition. This highlights the advantage of our distributed BESS control approach.

VI. Conclusion

A dual-consensus-based distributed control approach has been presented for frequency regulation in power systems with distributed BESSs. It consists of three main components in our design for BESS control gain, distributed BESS control strategy, and BESS parameter estimation, respectively. In the BESS parameter estimation, a static parameter and a time-varying parameter have been defined to enable implementation of our control strategy. Their average values are obtained by employing SAC and DAC, forming our dual-consensus approach. Case studies have been conducted to demonstrate the advantage of our approach. Future work includes investigating the effects of non-ideal communication links on the control performance, and merging other BESS functions such as energy arbitrage and reserve into distributed frequency control.

References

[1] National Grid ESO, "National electricity transmission system security and quality of supply standard version 2.3," Security and Quality of Supply Standard, Warwick, UK, Feb 2017.

[2] F. Teng, Y. Mu, H. Jia, J. Wu, P. Zeng, and G. Strbac, "Challenges of primary frequency control and benefits of primary frequency response support from electric vehicles," *Energy Procedia*, vol. 88, pp. 985–990, 2016.

[3] P. Mercier, R. Cherkaoui, and A. Oudalov, "Optimizing a battery energy storage system for frequency control application in an isolated power system," *IEEE Trans. Power Syst.*, vol. 24, no. 3, pp. 1469–1477, 2009.

[4] S. Zhang, Y. Mishra, and M. Shahidehpour, "Fuzzy-logic based frequency controller for wind farms augmented with energy storage systems," *IEEE Trans. Power Syst.*, vol. 31, no. 2, pp. 1595–1603, 2016.

[5] M. L. Lazarewicz and T. M. Ryan, "Integration of flywheel-based energy storage for frequency regulation in deregulated markets," in *IEEE Power and Energy Society General Meeting*, pp. 1–6, 2010.

[6] Y. Chen, M. Keyser, M. H. Tackett, and X. Ma, "Incorporating short-term stored energy resource into midwest iso energy and ancillary service market," *IEEE Trans. Power Syst.*, vol. 26, no. 2, pp. 829–838, 2011.

[7] Y. Cheng, M. Tabrizi, M. Sahni, A. Povedano, and D. Nichols, "Dynamic available agc based approach for enhancing utility scale energy storage performance," *IEEE Trans. Smart Grid*, vol. 5, no. 2, pp. 1070–1078, 2014.

[8] C. A. Hill, M. C. Such, D. Chen, J. Gonzalez, and W. M. Grady, "Battery energy storage for enabling integration of distributed solar power generation," *IEEE Trans. Smart Grid*, vol. 3, no. 2, pp. 850–857, 2012.

[9] S. Chen, T. Zhang, H. B. Gooi, R. D. Masiello, and W. Katzenstein, "Penetration rate and effectiveness studies of aggregated bess for frequency regulation," *IEEE Transactions on Smart Grid*, vol. 7, no. 1, pp. 167–177, 2016.

[10] D. Zhu and Y. J. Zhang, "Optimal coordinated control of multiple battery energy storage systems for primary frequency regulation," *IEEE Trans. Power Syst.*, 2018.

[11] K. Worthmann, C. M. Kellett, P. Braun, L. Grüne, and S. R. Weller, "Distributed and decentralized control of residential energy systems incorporating battery storage," *IEEE Trans. Smart Grid*, vol. 6, no. 4, pp. 1914–1923, 2015.

[12] G. N. Psarros, E. Karamanou, and S. A. Papathanassiou, "Feasibility analysis of centralized storage facilities in isolated grids," *IEEE Trans. Sustainable Energy*, 2018.

[13] B. M. Gundogdu, S. Nejad, D. T. Gladwin, M. Foster, and D. Stone, "A battery energy management strategy for uk enhanced frequency response and triad avoidance," *IEEE Trans. Ind. Electron.*, 2018.

[14] J. W. Shim, G. Verbič, K. An, J. H. Lee, and K. Hur, "Decentralized operation of multiple energy storage systems: Soc management for frequency regulation," in *IEEE Int. Conf. Power Syst. Techn. (POWERCON)*, pp. 1–5, 2016.

[15] W. Huang and J. A. A. Qahouq, "Energy sharing control scheme for state-of-charge balancing of distributed battery energy storage system," *IEEE Trans. Ind. Electron.*, vol. 62, no. 5, pp. 2764–2776, 2015.

[16] X. Lu, K. Sun, J. M. Guerrero, J. C. Vasquez, and L. Huang, "Double-quadrant state-of-charge-based droop control method for distributed energy storage systems in autonomous dc microgrids," *IEEE Trans. Smart Grid*, vol. 6, no. 1, pp. 147–157, 2015.

[17] H. Cai and G. Hu, "Distributed control scheme for package-level state-of-charge balancing of grid-connected battery energy storage system," *IEEE Trans. Ind. Inform.*, vol. 12, no. 5, pp. 1919–1929, 2016.

[18] X. Lu, K. Sun, J. M. Guerrero, J. C. Vasquez, and L. Huang, "State-of-charge balance using adaptive droop control for distributed energy storage systems in dc microgrid applications," *IEEE Trans. Ind. Electron.*, vol. 61, no. 6, pp. 2804–2815, 2014.

[19] R. Olfati-Saber and R. M. Murray, "Consensus problems in networks of agents with switching topology and time-delays," *IEEE Trans. Autom. Contr.*, vol. 49, no. 9, pp. 1520–1533, 2004.

[20] R. A. Freeman, P. Yang, and K. M. Lynch, "Stability and convergence properties of dynamic average consensus estimators," in *45th IEEE Conf. Decision and Control (CDC)*, pp. 338–343, 2006.

[21] S. Aditya and D. Das, "Application of battery energy storage system to load frequency control of an isolated power system," *Int. J. Energy Res.*, vol. 23, no. 3, pp. 247–258, 1999.

[22] C. Peng, J. Li, and M. Fei, "Resilient event-triggering h_∞ load frequency control for multi-area power systems with energy-limited dos attacks," *IEEE Trans. Power Syst.*, vol. 32, no. 5, pp. 4110–4118, 2017.

[23] D. Kottick, M. Blau, and D. Edelstein, "Battery energy storage for frequency regulation in an island power system," *IEEE Trans. Energy Conversion*, vol. 8, no. 3, pp. 455–459, 1993.

[24] A. Cooke, D. Strickland, and K. Forkasiewicz, "Energy storage for enhanced frequency response services," in *52nd Int. Universities Power Eng. Conf. (UPEC)*, pp. 1–6, 2017.

[25] D. Greenwood, K. Y. Lim, C. Patsios, P. Lyons, Y. S. Lim, and P. Taylor, "Frequency response services designed for energy storage," *Applied Energy*, vol. 203, pp. 115–127, 2017.

[26] C. Li, E. A. A. Coelho, T. Dragicevic, J. M. Guerrero, and J. C. Vasquez, "Multiagent-based distributed state of charge balancing control for distributed energy storage units in ac microgrids," *IEEE Trans. Ind. Appl.*, vol. 53, no. 3, pp. 2369–2381, 2017.

[27] P. Tabuada, "Event-triggered real-time scheduling of stabilizing control tasks," *IEEE Trans. Autom. Contr.*, vol. 52, no. 9, pp. 1680–1685, 2007.

Lantao Xing received the Ph.D. degree from Zhejiang University, China, in 2018. During 2015.09-2016.09, he was a visiting scholar at Nanyang Technological University, Singapore. He is currently a Research Fellow with the School of Electrical Engineering and Computer Science, Queensland University of Technology, Brisbane QLD, Australia. His research interests include nonlinear system control, distributed frequency control and smart grid.

Yateendra Mishra (S'06, M'09) received the Ph.D. degree from the University of Queensland, Brisbane, Australia, in 2009. He is currently a Senior Lecturer and Advanced QLD Research Fellow with the School of Electrical Engineering and Computer Science, Queensland University of Technology, Brisbane QLD, Australia. His research interests include distributed generation and distributed energy storage, and power system stability and control and their applications in smart grid.

Yu-Chu Tian (M'00) received the Ph.D. degree in computer and software engineering from the University of Sydney, Sydney NSW, Australia, in 2009 and the Ph.D. degree in industrial automation from Zhejiang University, Hangzhou, China, in 1993. He is currently a Professor in Computer Science with the School of Electrical Engineering and Computer Science, Queensland University of Technology, Brisbane QLD, Australia. His research interests include big data computing, distributed computing, cloud computing, computer networks, and control systems.

Gerard Ledwich (SM'89) received the Ph.D. degree in electrical engineering from the University of Newcastle, Newcastle, Australia, in 1976. He is a Chair Professor in Electrical Asset Management with the School of Electrical Engineering and Computer Science, Queensland University of Technology, Brisbane QLD, Australia. His research interests are in the areas of power systems, power electronics, and wide area control of smart grid.

Hongye Su (SM'14) received the B.E. degree in industrial automation from Nanjing University of Chemical Technology, Jiangsu, China, in 1990, and the M.E. and Ph.D. degrees from Zhejiang University, Hangzhou, China, in 1993 and 1995, respectively. He is a Professor with the Institute of Cyber-Systems and Control, Zhejiang University, Hangzhou, China. His research interests include robust control, time-delay systems, and advanced process control theory and applications.

Chen Peng (SM'15) received the M.E. and Ph.D. degrees from the Chinese University of Mining Technology, Xuzhou, China, in 1999 and 2002, respectively. He is currently a Professor with the School of Mechatronic Engineering and Automation, Shanghai University, Shanghai, China. His research interests are in the areas of networked control systems, power systems, fuzzy control systems, and interconnected systems.

Minrui Fei received the B.E. and M.E. degrees in industrial automation from the Shanghai University of Technology, Shanghai, China, in 1984 and 1992, respectively, and the Ph.D. degree in control theory and control engineering in 1997 from Shanghai University, Shanghai, China, where he has been a Full Professor since 1998. His research interests include networked control systems, intelligent control, complex system modeling, hybrid network systems, and field control systems.